Cancer Science
The official journal of the Japanese Cancer Association

αB-crystallin: A novel p53-target gene required for p53-dependent apoptosis

Gou Watanabe,[1,2] Shunsuke Kato,[1] Hideyuki Nakata,[1] Takanori Ishida,[2] Noriaki Ohuchi[2] and Chikashi Ishioka[1,3]

[1]Department of Clinical Oncology, Research Institute of Development, Aging and Cancer, Tohoku University, Sendai; [2]Division of Surgical Oncology, Tohoku University School of Medicine, Sendai, Japan

(Received April 20, 2009/Revised August 06, 2009/Accepted August 12, 2009/Online publication October 1, 2009)

The p53 protein is a transcription factor that *trans*-activates various genes in response to DNA-damaging stress. To search for new p53-target genes, we applied a cDNA microarray system using two independent p53-inducible cell lines, followed by *in silico* analysis to detect p53 response elements. Here, we report on crystallin alpha B gene (*CRYAB*), which encodes αB-crystallin, and is one of the genes directly *trans*-activated by p53. We confirmed it is directly transcribed by p53 using promoter analysis, deletion reporter assay, ChIP assay and EMSA. αB-crystallin is also upregulated in a p53-dependent manner and binds to the DNA-binding domain of p53. Overexpression of αB-crystallin increased p53 protein and, in contrast, repression of αB-crystallin decreased p53 protein. Interestingly, both overexpression and repression of αB-crystallin reduced p53-dependent apoptosis. In conclusion, we identified that αB-crystallin was a novel p53-target gene and required for p53-dependent apoptosis using two independent p53-inducible cell lines. This is the first report associating p53 directly with a heat shock protein through *trans*-activation and physical interaction. (*Cancer Sci* 2009; 100: 2368–2375)

Mutations in the *TP53* gene are the most frequent genetic alterations in various human tumors[1] and a large number of *TP53* mutations are reported in two major databases.[2,3] *TP53* encodes the p53 tumor suppressor, a 393-amino acid transcriptional activator comprising an N-terminal *trans*-activation domain, a sequence-specific DNA-binding domain, and a C-terminal tetramerization domain. Many of the *TP53* mutations found in tumors are missense mutation (approximately 75%) and are clustered in the core DNA-binding domain. Our previous study, based on functional analysis of 2314 p53 missense mutations, indicated that deactivation of p53 sequence specific *trans*-activation is likely to be critical for tumor development.[4,5] p53 plays a central role in maintaining genomic stability. Under genotoxic stress, p53 undergoes various post-translational modifications, such as phosphorylation and acetylation of a subset of residues, resulting in an oligomerized active form.[6] Oligomerized p53 binds to two copies of the specific consensus DNA sequence in the promoter region of p53 downstream genes and *trans*-activates them.[7] Many p53 downstream genes are identified by high-throughput technology such as cDNA microarray systems.[8]

αB-crystallin is the major structural protein of the eye lens and also a member of the small heat shock protein family.[9] It also functions as a molecular chaperone in lens fiber cells. It prevents thermally induced aggregation and plays an important role in maintaining lens transparency with αA-crystallin.[10] In contrast to the lens-specific expression of αA-crystallin, αB-crystallin is expressed in various tissues, although the level of expression is very low.[11–13] The extralenticular function of αB-crystallin remains unknown. Strict control of αB-crystallin levels is critical for normal development and maintenance of these cells, and has been shown to be associated with several neurological diseases[14–16] and malignant neoplasms.[17–19]

In order to search for new p53-target genes, we established two independent p53-inducible cell lines with different genetic backgrounds to eliminate individual variability, and identified that crystallin alpha B gene (*CRYAB*) is one of the p53-target genes that encodes αB-crystallin. p53 directly *trans*-activates *CRYAB* and induces αB-crystallin expression. αB-crystallin binds directly to the p53 DNA-binding domain and influences on p53 stability. Surprisingly, p53-dependent apoptosis is repressed by knockdown of αB-crystallin, which is known to be an anti-apoptotic protein. Our results indicate αB-crystallin expression is required for complete activity of p53-dependent apoptosis. This is the first report that p53 directly associates with a heat shock protein through both *trans*-activation and physical interaction.

Materials and Methods

Cell culture. Human cell lines Saos-2 (osteosarcoma, $TP53^{-/-}$), SF126 (glioblastoma, $TP53^{-/-}$), U2OS (osteosarcoma, $TP53^{+/+}$), and MCF-7 (breast cancer, $TP53^{+/+}$) were cultured in RPMI-1640 with 10% FCS at 37°C.

Expression plasmids. The wild-type p53 expression vector, pCR259-p53 and pcDNA5/TO-p53 were described previously.[4,20] The αB-crystallin expression vector (pCR259-cryab) was constructed by inserting them into the *EcoRI/EagI* site of a pCR259 vector. pcDNA5/TO-cryab and HA-cryab were constructed by inserting an αB-crystallin cDNA into a pcDNA5/TO vector or a modified pcDNA5/TO vector in which the HA epitope was inserted upstream of the multiple cloning site, respectively. The PCR primers for the αB-crystallin cDNA are shown in Supporting information Fig. S1. Flag-tagged p53 expression vectors were constructed using p3 × Flag-CMV-14vector (Sigma-Aldrich, St Louis, MO, USA) as described previously.[21] We named these constructs Flag-p53 (full-length p53), Flag-p53N (N-terminus of p53, residues 1–73), Flag-p53M (DNA-binding domain, residues 100–290), and Flag-p53C (C-terminus of p53, residues 290–393).

p53 inducible cell lines. pcDNA6/TR (Invitrogen, Carlsbad, CA, USA) was transfected into Saos2 or SF126 cells and selected at 10 μg/mL blasticidin. After 4 weeks selection, stable integration of pcDNA6/TR was confirmed by β-galactosidase assay in the selected stable clones (Saos2 TR or SF126 TR). pcDNA5/TO-p53 was transfected into these clones and selected for 4 weeks at 100–200 μg/mL hygromycin B. Tetracycline-dependent induction of p53 was confirmed in the established tetracycline inducible clones, Saos2-tet-p53 or SF126-tet-p53 by immunoblotting.

RNAi-mediated stable knockdown of αB-crystallin in SF126-tet-p53 or U2OS. αB-crystallin RNAi-oligonucleotide, described

[3]To whom correspondence should be addressed.
E-mail: chikashi@idac.tohoku.ac.jp

doi: 10.1111/j.1349-7006.2009.01316.x

previously,[22] was subcloned into a pBAsi-hH Neo DNA vector (Takara, Shiga, Japan). The resulting pBAsi-hH Neo vector (pBAsi) or pBAsi-αB-crystallin RNAi (pBAsi-cryab) was transfected in SF126-tet-p53 or U2OS and selected for 4 weeks at 500–700 μg/mL G418 (Roche Diagnostics, Indianapolis, IN, USA). Finally, αB-crystallin knockdown cell lines (SF126-tet-p53-pBAsi-cryab1 and cryab2, U2OS-pBAsi-cryab) and control cell lines (SF126-tet-p53-pBAsi1 and pBAsi2, U2OS-pBAsi) were obtained.

Microarray analysis. SF126-tet-p53 or Saos2-tet-p53 were grown to 70% confluence on 10 cm dishes, and further incubated with or without 10 ng/mL doxycycline for 24 h. Total RNA was extracted using a QIAamp RNA mini (Qiagen, Valencia, CA, USA). Comprehensive mRNA expression analysis was done using an AceGene (Human oligo chip 30K; Ace gene, Hitachisoft, Tokyo, Japan).

Real-time quantitative RT-PCR. cDNA was generated from 5 μg total RNA, extracted using an RNeasy Micro kit (Qiagen) from each sample by using the SuperScript II RNase H reverse transcriptase (Invitrogen). Real-time PCR was carried out in duplicate using a QuantiTect SYBR Green PCR kit (Qiagen). Reactions were analyzed on an Mx4000 (Stratagene, La Jolla, CA, USA) using a fluorescence threshold corresponding to the middle of the exponential range. Two internal controls, *GAPDH* and *ACTB* (a gene encoding β-actin), were used to adjust the data. Real-time PCR primers used in this study are listed in Supporting information Fig. S1.

***In silico* analysis of *CRYAB* promoter.** To search for putative p53 response elements in the *CRYAB* gene promoter, we used the p53 Scanner program (http://bioinformatics.wistar.upenn.edu/P53), which uses a position-weight matrix to identify putative p53 response elements in a given DNA sequence highly conserved in both the mouse and human genomes.

Protein preparation and immunoblot analysis. Whole cell lysate was obtained using an SDS-containing buffer as described previously.[22] The lysate was analyzed by Western blotting as described previously[23] using anti-p53 (FL393:sc-6234 HRP; Santa Cruz Biotechnology, Santa Cruz, CA, USA), anti-αB-crystallin (SPA-222 and SPA-223; Stressgen Biotechnology, Ann Arbor, MI, USA), anti-β-actin (ab8226; Abcam, Cambridge, MA, USA), anti-HA (HA.11.:MMS-101R; Covance, Princeton, NJ, USA) and anti-FLAG (M2:F3165; Sigma-Aldrich) antibodies.

Dual luciferase assay. For reporter constructs, five distinct DNA fragments containing ~1.48 kb of the 5′-flanking region of the *CRYAB* gene were isolated by human genomic PCR and subsequently subcloned into a pGL3E-basic vector.[20] The PCR primers are listed in Supporting information Fig. S1. SF126 cells 1×10^4 were seeded in tetraplicate into 96-well tissue culture plates (Coster 3917; Corning, NY, USA) and the following plasmids were transfected into the cells with FuGENE 6 (Roche Applied Science, Indianapolis, IN, USA). For each well, 50 ng of reporter construct was co-transfected with 10 ng pCR259-p53 or pCR259 and with 5 ng *Renilla* luciferase control vector pRL-CMV (Promega, Madison, WI, USA). Twenty-four hours after transfection, reporter activities were analyzed using the Dual-Glo Luciferase Assay System kit (Promega) and were measured by a 96-well formatted Fluoroskan Ascent FL fluorometer (Labsystems, Helsinki, Finland). To correct for variation in transfection efficiency, reporter firefly luciferase activity was normalized to *Renilla* luciferase activity.

ChIP assay. pCR259-p53 was transfected in SF126 using FuGENE6. Twenty-four hours after transfection, the cells were treated with 1% formaldehyde for 10 min at 37°C. The assay was carried out using a ChIP assay kit (Millipore, Billerica, MA, USA) according to the manufacturer's instruction, using anti-p53 (FL393) antibody or anti-rabbit IgG (as a negative control) for immunoprecipitation and *CRYAB* promoter-specific PCR primers listed in Supporting information Fig. S1.

Immunoprecipitation assay. SF126 cells were grown to 60% confluence on 10 cm tissue culture dishes. Flag-p53 (2 μg), HA-cryab (4 μg), or pCR259 (to adjust the total quantity to 6 μg plasmid) were co-transfected with or without each plasmid as indicated. U2OS cells, for endogenous interaction, were grown to 80% confluence on 10 cm culture dishes and after 24 h, were treated or not treated with UV light, 20 J/m^2. Twenty-four hours after the transfection, immunoprecipitation was carried out according to the method described previously[24] using an anti-HA or anti-Flag antibody.

Fig. 1. Multidisciplinary methods to identify novel p53-target genes. Two p53-null cell lines, Saos2 and SF126, were stably integrated with pcDNA6/TR vector and pcDNA5/TO-p53 (p53 expression vector). Microarray technology was applied to the established p53-inducible cell lines, Saos2-tet-p53 and SF126-tet-p53, for the selection of p53-target genes.

Table 1. Common p53-inducible genes between Saos2-tet-p53 and SF126-tet-p53 cells

Symbol name	Relative expression (p53+/p53–)
TP53I3†	8.73
PLAB†	7.26
PIR121†	6.75
GADD45†	5.8
GNS	4.86
CTGF	4.74
C12orf5	4.07
MABA1	3.59
MKP6	3.57
CRYAB	3.56
hspc141	3.42
C20orf11	3.19
TM7SF6	2.93
annexin A4	2.93
TNFRSF6†	2.88
spermidine	2.87
hspc132†	2.78
POLH†	2.65
loc91412	2.64
DDB2†	2.54
RPS27L	2.53
PVT1	2.48
caveolin 1	2.36
THSD1	2.32
syntaxin 6	2.3
ATP6AP2	2.29
NAD synthetase 1	2.1
PNUTL2†	2.08
BTG2†	2.06
C21orf62	2.04
FHL2†	2.01

†Previously described p53-inducible genes (including indirect target genes).

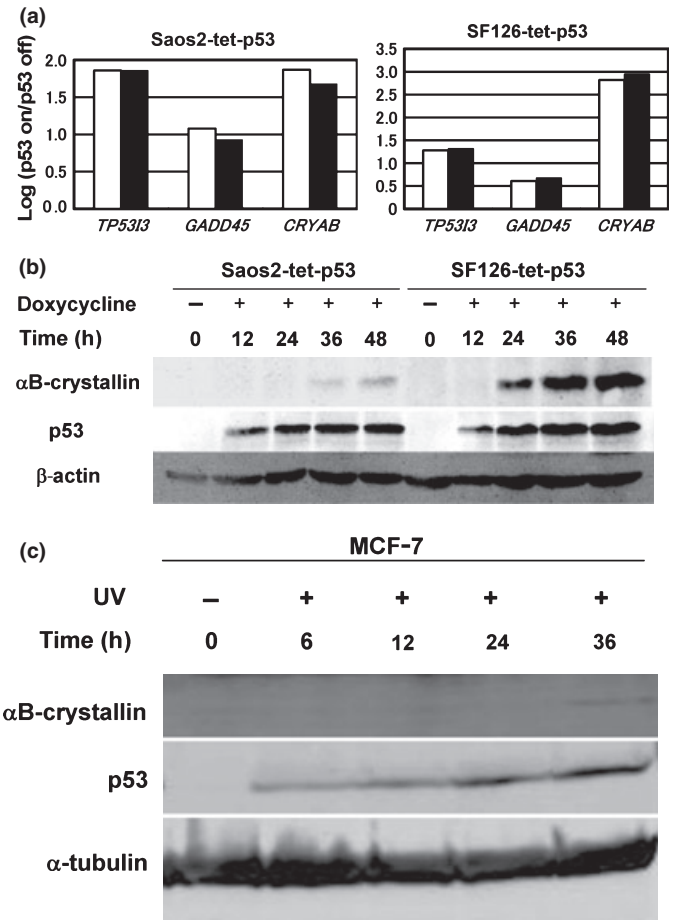

Fig. 2. p53-Dependent induction of crystallin alpha B (*CRYAB*) mRNA and αB-crystallin. (a) Expression of *CRYAB* mRNA levels relative to two internal controls, *GAPDH* (open bar) or β-actin (filled bar) by quantitative RT-PCR in Saos2-tet-p53 and SF126-tet-p53 cell lines. *TP53I3* and *GADD45* genes were used as positive controls. (b) p53-Dependent induction of αB-crystallin in Saos2-tet-p53 and SF126-tet-p53 cell lines detected by immunoblotting. (c) p53-Dependent induction of endogenous αB-crystallin in MCF-7 breast cancer cells treated with UV light, 60 J/m^2 detected by immunoblotting.

Cell viability assay. Two independent αB-crystallin knockdown cell lines or control cell lines were seeded in 96-well plates (1×10^4cells/well) and incubated with or without 5 ng/mL doxycycline for p53 induction. Cells were maintained in further incubation at 37°C for 0, 24, or 48 h. Cell proliferation assay were carried out with a Cell Counting Kit-8 (Dojin Laboratories, Kumamoto, Japan) according the manufacturer's instructions. Absorbance at each indicated time relative to 0 h absorbance was calculated as a relative absorbance score.

FACS. SF126-tet-p53-pBAsi-cryab and SF126-tet-p53-pBAsi were incubated with or without 5 ng/mL doxycycline for 48 h. 3×10^5 SF126 cells were analyzed for FACS as described previously.[23] Among three plasmids pCR259 (0.5∼2.0 μg), pCR259-p53 (0.5 μg) and pCR259-cryab (1.5 μg), two distinct plasmids (total DNA quantity to 2 μg) were co-transfected into 3×10^5 parent SF126 cells, incubate for 48 h and analyzed for FACS.

Results

Strategy to identify novel p53-target genes. To determine novel p53 downstream genes, we established tetracycline-dependent p53-inducible cells derived from the two p53-null cell lines, Saos2-tet-p53 and SF126-tet-p53 (Fig. 1). Using a DNA microarray, we determined 31 *trans*-activating genes (Table 1), for which the mRNA levels were twice as high in the p53 induced condition than in the p53 uninduced condition. Of the 31 genes, 11 are already known as p53-inducible genes. The remaining 20 genes are novel p53-target gene candidates. We searched for p53 response elements in the 20 genes and *CRYAB* was the only candidate gene of a novel p53-target.

αB-crystallin induced by p53. To confirm that *CRYAB* mRNA is upregulated by p53 expression, quantitative RT-PCR was carried out (Fig. 2a). p53-mediated induction of the *CRYAB* mRNA was approximately four and eight times higher in Saos2-tet-p53 and SF126-tet-p53 cells, respectively. These are sufficient inductions compared with positive control genes *TP53I3* and *GADD45*. Moreover, the induction of αB-crystallin was both p53-dependent and time-dependent (Fig. 2b). To examine whether αB-crystallin was also induced by UV damage, MCF-7 cells harboring endogenous wild-type p53 were treated with UV. As shown in Figure 2c, αB-crystallin was induced after UV damage, following p53 expression. *CRYAB* mRNA is also induced by UV damaged MCF-7, harboring endogenous p53, but under the p53 knockdown status using p53 siRNA, the *CRYAB* mRNA expression level is decreased (Supporting information Fig. S2). These results indicated that both *CRYAB* mRNA and αB-crystallin protein were upregulated under the conditions

doi: 10.1111/j.1349-7006.2009.01316.x

of both tetracycline-inducible exogenous p53 and stress-inducible endogenous p53. Therefore, we concluded that *CRYAB* was a candidate p53-target gene.

p53 *trans*-activates *CRYAB* directly. Using the p53 Scanner program, we identified two putative p53 response elements, p53RE1 and p53RE2, in the intronic region, −208/−188 and −106/−72, respectively, upstream of the transcription initiation site of *CRYAB* (Fig. 3a). To evaluate whether these elements were truly activated by p53 *in vivo*, we carried out a luciferase assay for DNA fragments containing 0.18–1.48 kb of the 5′-flanking region of the *CRYAB* gene (Cryab-P1–P5; Fig. 3b). When p53 was expressed in SF126 cells, luciferase activity was retained until the p53RE1 was removed, whereas no luciferase activity was observed in the Cryab-P1 fragment with p53RE2 alone (Fig. 3c). These results show that p53RE1 acts as a p53 response element *in vivo*. To determine whether p53 binds directly to p53RE1 *in vivo*, we carried out a ChIP assay using a *CRYAB*-specific primer and a *CDKN1A*-specific primer as positive controls. As shown in Figure 3d, the *CRYAB* gene was specifically immunoprecipitated with an anti-p53 antibody and amplified by PCR. We also confirmed that p53 binds p53RE1 *in vitro* by EMSA (Supporting information Fig. S3) and these results indicate that the binding of p53 to p53-RE1 in the *CRYAB* gene is specific. We concluded that *CRYAB* is directly *trans*-activated by p53 through a p53-responsive element in the *CRYAB* promoter.

αB-crystallin binds to p53 DNA-binding domain. To investigate the physical interaction between αB-crystallin and p53, we carried out an immunoprecipitation assay. An HA-tagged αB-crystallin and a Flag-tagged p53 were expressed in p53-null SF126 cells and immunoprecipitated by anti-HA or anti-Flag antibodies. In Figure 4a, αB-crystallin and p53 forms a complex, as reported previously.[25] Moreover, when U2OS cells were treated with UV, the interaction between the endogenous p53 and αB-crystallin was also observed (Fig. 4b). We also carried out immunostaining of p53 and αB-crystallin (Supporting information Fig. S4). Although the majority of αB-crystallin was localized in cytosol, small fractions of αB-crystallin were in the nucleus and co-localized with p53. Finally, to determine the specific binding domain of p53 for αB-crystallin, Flag-tagged NH_2-domain, a DNA-binding domain, and a COOH domain of p53 and αB-crystallin were co-expressed in SF126 cells and immunoprecipitated by an anti-Flag antibody. Because the expression levels of three domains were different, and therefore, it was difficult to evaluate interaction of αB-crystallin to these domains quantitatively. αB-crystallin seems to bind to p53 at least through the DNA-binding domain (Fig. 4c). Because αB-crystallin also works as a chaperone,[10] it might support the folding of the hydrophobic p53 DNA-binding domain.

αB-crystallin influence on p53 stability. We next asked whether αB-crystallin expression levels would influence p53 function. To elucidate the physiological significance of αB-crystallin

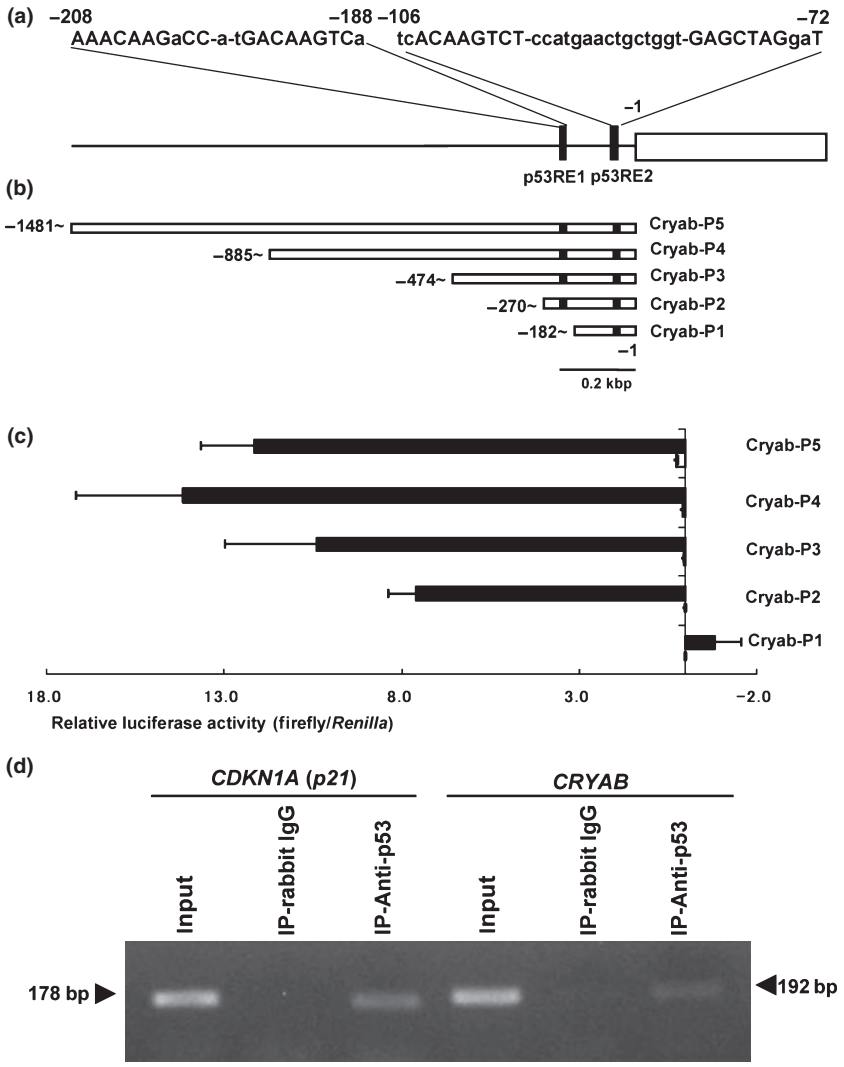

Fig. 3. Crystallin alpha B (*CRYAB*) is directly *trans*-activated by p53. (a) Schematic representation of the *CRYAB* 5′ promoter region. Black boxes represent putative p53 response elements p53RE1 and p53RE2. Capital letters indicate p53 consensus binding sequence. (b) Schematic representation of reporter plasmids. Both (a) and (b), numbers indicate relative position to the transcription initiation site. (c) Promoter activity of *CRYAB* gene. p53-Dependent *trans*-activity through the indicated promoter construct was measured by dual luciferase assay. Filled bar, p53 expression; open bar, p53 null. Values shown are mean ± SD ($n = 4$). (d) p53 binds to *CRYAB* promoter region *in vivo*. Chromatin immunoprecipitation assay was carried out with p53 antibody or anti-rabbit IgG after p53 expression plasmid transfection. Numbers indicate the size of PCR products for *CDKN1A* (*p21*) (left) and *CRYAB* (right). IP, immunoprecipitation.

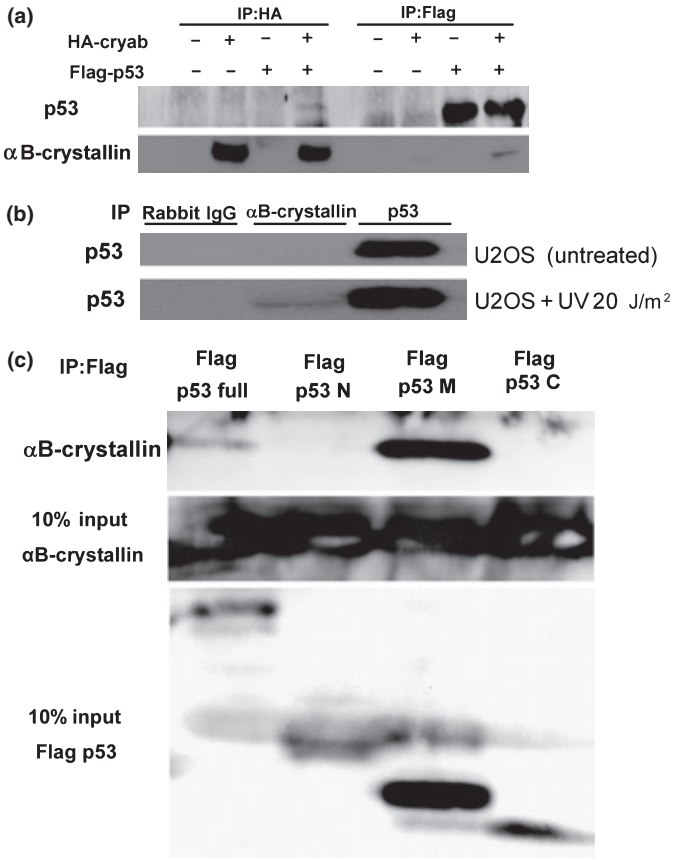

Fig. 4. αB-crystallin binds to p53 DNA-binding domain. (a) Immunoprecipitation assay of HA-tagged αB-crystallin and Flag-tagged p53 in SF126 glioblastoma cells. Immunoblotting was carried out by anti-p53 or anti-αB-crystallin antibodies. IP, immunoprecipitation. (b) Endogenous αB-crystallin and p53 form complexes in UV-treated U2OS osteosarcoma cells. Immunoblot assay was carried out by anti-p53 antibody. (c) αB-crystallin interactive domain of p53. HA-tagged αB-crystallin and Flag-tagged full-length p53 or indicated p53 domains were expressed in SF126 cells. Immunoprecipitation assay was carried out using anti-Flag antibody and immunoblotted by anti-αB-crystallin antibody.

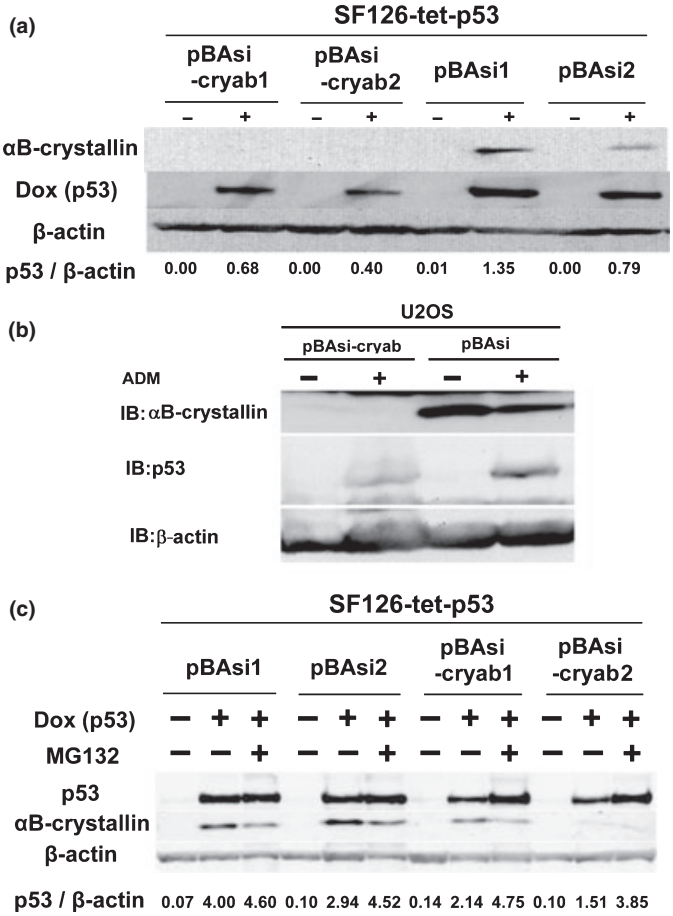

Fig. 5. αB-crystallin stabilized p53. (a) Stable knockdown of αB-crystallin cell lines, SF126-tet-p53-pBAsi-cryab1 and 2 (pBAsi-cryab1 and pBAsi-cryab2), and control cell lines, SF126-tet-p53-pBAsi1 and 2, were incubated for 36 h with or without 5 ng/mL doxycycline (Dox). After incubation, the cell lysates were immunoblotted by p53 or αB-crystallin antibodies. (b) A stable knockdown of αB-crystallin cell line, U2OS-pBAsi-cryab, and a control cell line, U2OS-pBAsi were incubated for 24 h with or without 0.1 μM adriamycin (ADM). IB, immunoblotting. (c) Cell lines used in (a) were incubated for 36 h with or without Dox and were further incubated for 12 h with or without 30 nM of proteasome inhibitor MG132.

induced by p53, we established αB-crystallin stable knockdown or control clones in the p53-inducible cell line, SF126-tet-p53. In the αB-crystallin knockdown clones (SF126-tet-p53-pBAsi-cryab1 and -cryab2), the expression of αB-crystallin protein was completely repressed (Fig. 5a). Interestingly, p53 protein levels were also decreased by approximately 50% by αB-crystallin knockdown. To exam whether αB-crystallin also stabilizes endogenous p53, we also constructed an αB-crystallin knockdown U2OS cell line, U2OS-pBAsi-cryab, and a control cell line, U2OS-pBAsi. Adding DNA damage to these cell lines with adriamycin, p53 protein is induced in both, but the p53 expression level is downregulated in the U2OS-pBAsi-cryab cell line (Fig. 5b). Furthermore, the proteasome inhibitor MG132 recovered the decreased protein level of p53 in p53 knockdown cell lines (Fig. 5c). These data suggest that αB-crystallin supports the p53 proper folding and contributes to p53 stability.

Overexpression and suppression of αB-crystallin interferes with p53-dependent inhibition of cell proliferation and apoptosis. p53-Dependent inhibition of cell proliferation and apoptosis are important for p53 functions. To investigate whether αB-crystallin is associated with these p53 functions, we examined the proliferation activities of αB-crystallin knockdown cell lines and control cell lines (Fig. 6a). Without p53 expression, both αB-crystallin knockdown cell lines and control cell lines grew equivalently. When p53 was expressed, the viabilities of both cell lines were markedly decreased. However, the reduction in cell viability was partially rescued in αB-crystallin repressed cell lines. To evaluate whether the αB-crystallin knockdown affects p53-dependent apoptosis, sub-G_1 in these cell lines was calculated by FACS. As shown in Figure 6b, p53-dependent apoptosis was repressed by αB-crystallin knockdown. These results indicated that p53-dependent inhibition of cell proliferation is due to p53-dependent apoptosis predominantly. But previous reports revealed that overexpression of αB-crystallin inhibits apoptosis.[26–30] In our system, p53-dependent apoptosis was also repressed by αB-crystallin overexpression (Fig. 6c). These results indicate that both overexpression and knockdown of αB-crystallin prevent apoptosis and the physiological protein level of αB-crystallin is necessary for p53-dependent apoptosis.

Discussion

Although a number of p53-target genes have been identified, several remain unidentified because there are a number of

doi: 10.1111/j.1349-7006.2009.01316.x

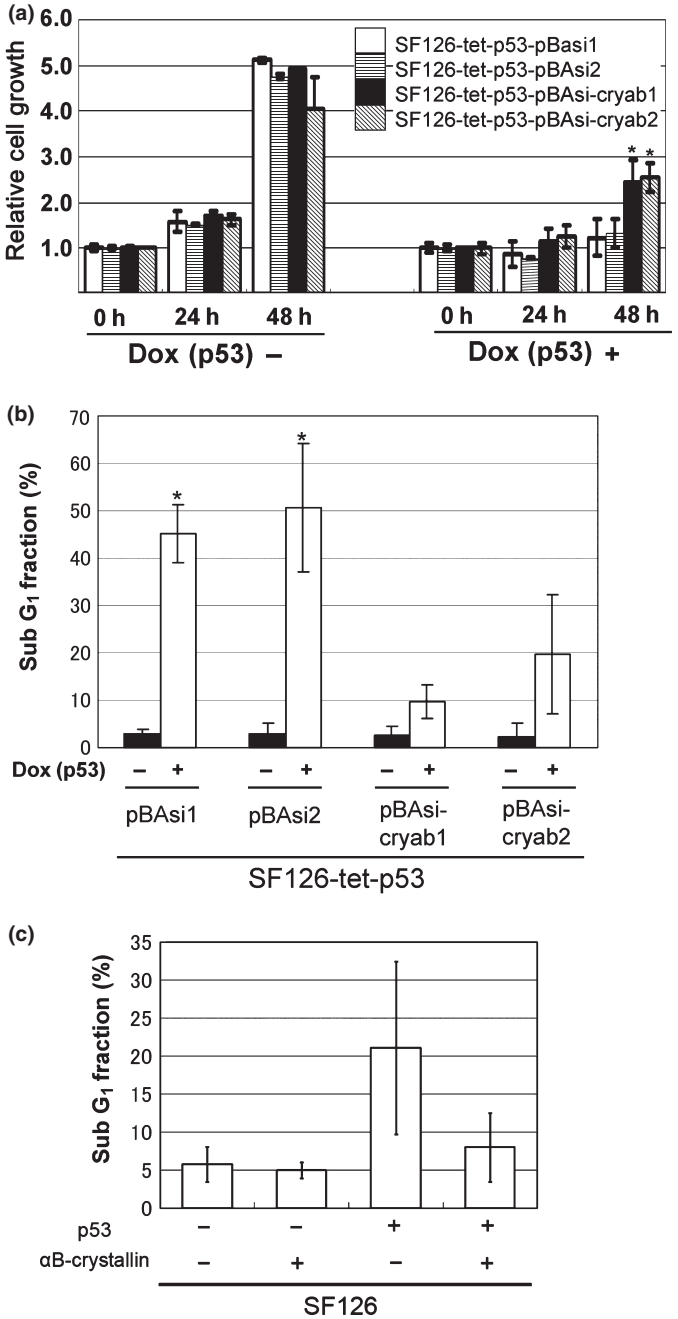

Fig. 6. Both repression and overexpression of αB-crystallin attenuates p53-dependent apoptosis. (a) SF126-tet-p53-pBAsi-cryab1 and 2, and control cell lines SF126-tet-p53-pBAsi1 and 2. Cells were treated with or without doxycycline (Dox) and cell viability assays were carried out (cell viability just before treatment = 1.0). Values shown are mean ± SD ($n = 3$). *$P < 0.01$ between αB-crystallin knockdown clone (pBAsi-cryab1 or pBAsi-cryab2) and control clone (pBAsi2) with Dox at 48 h. (b) p53-Dependent apoptosis were analyzed for sub G_1 fractions by FACS after 48 h with or without Dox (a). Values shown are mean ± SD ($n = 3$). *$P < 0.05$ between control clone (pBAsi1 or pBAsi2) and αB-crystallin knockdown clone (pBAsi-cryab2). (c) p53-Dependent apoptosis were analyzed for sub G_1 fractions by FACS in αB-crystallin overexpressed SF126 glioblastoma cells.

p53-binding sequences in the whole genome. Recently, systematic strategies such as screening p53-binding elements from the whole genome by an *in silico* sequence search[31] and an *in vitro* genome-wide ChIP screening for p53 binding[32,33] were adopted to identify novel p53-target genes. Another strategy is a comparative expression analysis of cells with and without p53 expression by DNA microarray technologies.[8,34] Although these methods are very powerful and useful, and pick up a number of candidate genes, they are not highly specific and have difficulty in identifying direct p53-target genes.

To avoid indirectly upregulated genes by p53 or non-specific genes unrelated to p53 functions, we used two inducible p53 cell lines with distinct genetic and histological backgrounds that permit a low level of p53 expression by minimizing doxycycline concentration, and compared their differentially expressed genes using the microarray strategy. We used the p53 Scanner to search p53 response elements among 20 candidate genes, and identified the *CRYAB* gene as a novel p53-target gene.

p53-Target genes encode proteins that are categorized to cell cycle control,[35,36] apoptosis,[37,38] and other cellular functions.[39,40] Among these, several particular proteins directly bind to p53, and often affect p53 function. MDM2 is one of the examples and diminishes p53 levels through ubiquitin ligase activity. Our and other previous studies have shown that αB-crystallin is also a p53-binding protein. In overexpressed conditions, Liu *et al.* suggested that αB-crystallin binds to p53 to sequester its translocation to mitochondria.[41] However, in physiological conditions, the function caused by αB-crystallin-p53 interaction remains unclear.

αB-crystallin is a member of the family of small heat shock proteins and acts as molecular chaperone.[10] Other heat shock proteins such as Hsp90, Hsp70, and mot-2 also interact with p53 and modulate p53 function by controlling stability and/or cellular distribution of p53.[42] Like p53, heat shock proteins are activated under various cellular stresses such as heat shock, hydrogen peroxide, heavy metals, or UV. Heat shock proteins also act as molecular chaperones, and maintain protein conformation and prevent protein aggregation. In this experiment, established αB-crystallin knockdown cell lines decreased both exogenous and endogenous expressed p53 protein levels. The decreased protein levels were restored by the addition of a proteasome inhibitor (Fig. 5). Furthermore, overexpression of αB-crystallin increases p53 protein levels in a dose-dependent manner (Supporting information Fig. S5). These results suggest that αB-crystallin might contribute to p53 stability. The interaction of a heat shock protein with p53 is considered to be a reasonable cellular function because p53 acts under stress conditions and should be protected by a heat shock protein.

αB-crystallin has been described as an anti-apoptotic regulator through, at least in part, inhibition of the p53-dependent apoptotic pathway.[26–30] αB-crystallin binds to Bax, also a p53-target gene product, and inhibits translocation of Bax to mitochondria and abrogates Bax-dependent apoptosis.[26] αB-crystallin also binds to pro-caspase3, a more common protein in the apoptosis pathway, and blocks pro-caspase3 proteolysis.[27–29] Moreover, αB-crystallin transforms immortalized human mammary epithelial cells and forms invasive mammary carcinomas in nude mice.[43] Although all these anti-apoptotic functions were conducted from experiments over-expressing αB-crystallin, we initially predicted that abrogation of endogenous αB-crystallin would enhance the p53-dependent apoptosis. Surprisingly, we obtained the inverse result: endogenous αB-crystallin expression is required for complete activity of p53-dependent apoptosis.

The precise mechanisms of both overexpression and knockdown αB-crystallin prevent from p53-dependent apoptosis are unknown. But the pro-apoptotic function of αB-crystallin is supported by the fact that αB-crystallin-deficient lens epithelial cells from knockout mice display phenotypes similar to human tumor cells with *TP53* mutation, even though the cells retain wild-type p53.[44] These phenotypes include hyper-proliferation of cells, and impairment of G_1 arrest after gamma-irradiation.

Our data may reflect that physiological levels of αB-crystallin protein work as a molecular chaperone in the cell and is needed for the proper function of p53. In contrast, overexpressed αB-crystallin prevents apoptosis, through the interaction of the p53 downregulated genes, such as *bax*,[38] or the more common apoptosis pathway protein, such as pro-caspase3.[39–42]

In conclusion, we identified *CRYAB* as a p53-target gene and showed that αB-crystallin, a product of the *CRYAB* gene, directly interacts with p53 and is necessary for p53-dependent apoptosis. Our study obtained three important findings. First, we established highly specific systems to identify target genes. Second, *CRYAB* is the first p53-target gene to be categorized as a heat shock protein. Finally, we showed that αB-crystallin acts as a pro-apoptotic protein rather than an anti-apoptotic protein in the p53 pathway under physiological conditions. Further studies are needed to elucidate the roles of αB-crystallin, especially in the p53 pathway and affecting p53 protein.

Acknowledgments

We thank Shin Takahashi, Satsuki Mashiko, and Atsuko Sato for their technical assistance. This study was supported by grants-in-aid from the Ministry of Education, Sciences, Sports, and Culture (12217010 and 17015002), and the Gonryo Medical Foundation to C.I.

References

1 Hollstein M, Rice K, Greenblatt MS *et al.* Database of p53 gene somatic mutations in human tumors and cell lines. *Nucleic Acids Res* 1994; **22**: 3551–5.
2 Hamroun D, Kato S, Ishioka C, Claustres M, Beroud C, Soussi T. The UMD TP53 database and website: update and revisions. *Hum Mutat* 2006; **27**: 14–20.
3 Olivier M, Eeles R, Hollstein M, Khan MA, Harris CC, Hainaut P. The IARC TP53 database: new online mutation analysis and recommendations to users. *Hum Mutat* 2002; **19**: 607–14.
4 Kato S, Han SY, Liu W *et al.* Understanding the function-structure and function-mutation relationships of p53 tumor suppressor protein by high-resolution missense mutation analysis. *Proc Natl Acad Sci USA* 2003; **100**: 8424–9.
5 Kawaguchi T, Kato S, Otsuka K *et al.* The relationship among p53 oligomer formation, structure and transcriptional activity using a comprehensive missense mutation library. *Oncogene* 2005; **24**: 6976–81.
6 Liu G, Chen X. Regulation of the p53 transcriptional activity. *J Cell Biochem* 2006; **97**: 448–58.
7 el-Deiry WS, Kern SE, Pietenpol JA, Kinzler KW, Vogelstein B. Definition of a consensus binding site for p53. *Nat Genet* 1992; **1**: 45–9.
8 Kho PS, Wang Z, Zhuang L *et al.* p53-regulated transcriptional program associated with genotoxic stress-induced apoptosis. *J Biol Chem* 2004; **279**: 21183–92.
9 Dubin RA, Ally AH, Chung S, Piatigorsky J. Human αB-crystallin gene and preferential promoter function in lens. *Genomics* 1990; **7**: 594–601.
10 Horwitz J. Alpha-crystallin can function as a molecular chaperone. *Proc Natl Acad Sci USA* 1992; **89**: 10449–53.
11 Iwaki T, Kume-Iwaki A, Goldman JE. Cellular distribution of αB-crystallin in non-lenticular tissues. *J Histochem Cytochem* 1990; **38**: 31–9.
12 Dubin RA, Wawrousek EF, Piatigorsky J. Expression of the murine αB-crystallin gene is not restricted to the lens. *Mol Cell Biol* 1989; **9**: 1083–91.
13 Bhat SP, Nagineni CN. αB subunit of lens-specific protein alpha-crystallin is present in other ocular and non-ocular tissues. *Biochem Biophys Res Commun* 1989; **158**: 319–25.
14 Iwaki T, Kume-Iwaki A, Liem RK, Goldman JE. αB-crystallin is expressed in non-lenticular tissues and accumulates in Alexander's disease brain. *Cell* 1989; **57**: 71–8.
15 Iwaki T, Wisniewski T, Iwaki A *et al.* Accumulation of αB-crystallin in central nervous system glia and neurons in pathologic conditions. *Am J Pathol* 1992; **140**: 345–56.
16 Lowe J, McDermott H, Pike I, Spendlove I, Landon M, Mayer RJ. αB crystallin expression in non-lenticular tissues and selective presence in ubiquitinated inclusion bodies in human disease. *J Pathol* 1992; **166**: 61–8.
17 Sorlie T, Perou CM, Tibshirani R *et al.* Gene expression patterns of breast carcinomas distinguish tumor subclasses with clinical implications. *Proc Natl Acad Sci USA* 2001; **98**: 10869–74.
18 Chelouche-Lev D, Kluger HM, Berger AJ, Rimm DL, Price JE. αB-crystallin as a marker of lymph node involvement in breast carcinoma. *Cancer* 2004; **100**: 2543–8.
19 Aoyama A, Steiger RH, Frohli E *et al.* Expression of αB-crystallin in human brain tumors. *Int J Cancer* 1993; **55**: 760–4.
20 Shimada A, Kato S, Enjo K *et al.* The transcriptional activities of p53 and its homologue p51/p63: similarities and differences. *Cancer Res* 1999; **59**: 2781–6.
21 Kastan MB, Zambetti GP. Parc-ing p53 in the cytoplasm. *Cell* 2003; **112**: 1–2.
22 Kamradt MC, Lu M, Werner ME *et al.* The small heat shock protein αB-crystallin is a novel inhibitor of TRAIL-induced apoptosis that suppresses the activation of caspase-3. *J Biol Chem* 2005; **280**: 11059–66.
23 Kakudo Y, Shibata H, Otsuka K, Kato S, Ishioka C. Lack of correlation between p53-dependent transcriptional activity and the ability to induce apoptosis among 179 mutant p53s. *Cancer Res* 2005; **65**: 2108–14.
24 Starita LM, Horwitz AA, Keogh MC, Ishioka C, Parvin JD, Chiba N. BRCA1/BARD1 ubiquitinate phosphorylated RNA polymerase II. *J Biol Chem* 2005; **280**: 24498–505.
25 Shuang Liu GD, Zizhi Tu, Junli Li, Medidong Liu, Xianzhong Xiao. The effect of αB-crystallin on mitochondrial death pathway during hydrogen peroxide induced apoptosis. *EXCLI J* 2005; **4**: 7–24.
26 Mao YW, Liu JP, Xiang H, Li DW. Human αA- and αB-crystallins bind to Bax and Bcl-X(S) to sequester their translocation during staurosporine-induced apoptosis. *Cell Death Differ* 2004; **11**: 512–26.
27 Li DW, Xiang H, Mao YW *et al.* Caspase-3 is actively involved in okadaic acid-induced lens epithelial cell apoptosis. *Exp Cell Res* 2001; **266**: 279–91.
28 Kamradt MC, Chen F, Cryns VL. The small heat shock protein αB-crystallin negatively regulates cytochrome c- and caspase-8-dependent activation of caspase-3 by inhibiting its autoproteolytic maturation. *J Biol Chem* 2001; **276**: 16059–63.
29 Kamradt MC, Chen F, Sam S, Cryns VL. The small heat shock protein αB-crystallin negatively regulates apoptosis during myogenic differentiation by inhibiting caspase-3 activation. *J Biol Chem* 2002; **277**: 38731–6.
30 Li DW, Liu JP, Mao YW *et al.* Calcium-activated RAF/MEK/ERK signaling pathway mediates p53-dependent apoptosis and is abrogated by αB-crystallin through inhibition of RAS activation. *Mol Biol Cell* 2005; **16**: 4437–53.
31 Maruyama R, Aoki F, Toyota M *et al.* Comparative genome analysis identifies the vitamin D receptor gene as a direct target of p53-mediated transcriptional activation. *Cancer Res* 2006; **66**: 4574–83.
32 Jen KY, Cheung VG. Identification of novel p53 target genes in ionizing radiation response. *Cancer Res* 2005; **65**: 7666–73.
33 Wei CL, Wu Q, Vega VB *et al.* A global map of p53 transcription-factor binding sites in the human genome. *Cell* 2006; **124**: 207–19.
34 Nakamura Y. Isolation of p53-target genes and their functional analysis. *Cancer Sci* 2004; **95**: 7–11.
35 el-Deiry WS, Tokino T, Velculescu VE *et al.* WAF1, a potential mediator of p53 tumor suppression. *Cell* 1993; **75**: 817–25.
36 Hermeking H, Lengauer C, Polyak K *et al.* 14-3-3 sigma is a p53-regulated inhibitor of G2/M progression. *Mol Cell* 1997; **1**: 3–11.
37 Miyashita T, Reed JC. Tumor suppressor p53 is a direct transcriptional activator of the human bax gene. *Cell* 1995; **80**: 293–9.
38 Nakano K, Vousden KH. PUMA, a novel proapoptotic gene, is induced by p53. *Mol Cell* 2001; **7**: 683–94.
39 Barak Y, Juven T, Haffner R, Oren M. mdm2 expression is induced by wild type p53 activity. *EMBO J* 1993; **12**: 461–8.
40 Dornan D, Wertz I, Shimizu H *et al.* The ubiquitin ligase COP1 is a critical negative regulator of p53. *Nature* 2004; **429** (6987): 86–92.
41 Liu S, Li J, Tao Y, Xiao X. Small heat shock protein αB-crystallin binds to p53 to sequester its translocation to mitochondria during hydrogen peroxide-induced apoptosis. *Biochem Biophys Res Commun* 2007; **354**: 109–14.
42 Zylicz M, King FW, Wawrzynow A. Hsp70 interactions with the p53 tumour suppressor protein. *EMBO J* 2001; **20**: 4634–8.
43 Moyano JV, Evans JR, Chen F *et al.* αB-crystallin is a novel oncoprotein that predicts poor clinical outcome in breast cancer. *J Clin Invest* 2006; **116**: 261–70.
44 Bai F, Xi JH, Wawrousek EF, Fleming TP, Andley UP. Hyperproliferation and p53 status of lens epithelial cells derived from αB-crystallin knockout mice. *J Biol Chem* 2003; **278**: 36876–86.

doi: 10.1111/j.1349-7006.2009.01316.x

Supporting Information

Additional Supporting Information may be found in the online version of this article:

Fig. S1. PCR primers and oligomers used in this study.

Fig. S2. (a) Quantitative RT-PCR of crystallin alpha B (*CRYAB*) using transiently knocked down p53 MCF-7 breast cancer cells. IB, immunoblotting. (b) MCF-7 cells were grown to 60% confluence on a six-well plate and 0.5 μg p53 siRNA or control siRNA (Santa Cruz Biotechnology, Santa Cruz, CA, USA) were transfected according to the manufacturer's protocol. After 24 h, these cells were treated or not treated with 60 J/m^2 of UV. A further 24 h after incubation, cells were harvested and mRNA extracted.

Fig. S3. Gel shift assay for p53RE1 in crystallin alpha B (*CRYAB*). Nuclear extracts were prepared from SF126-tet-p53 cells with or without 5 ng/mL doxycycline using NE-PER nuclear and cytoplasmic extraction reagents (Pierce, Rockford, IL, USA) according to the manufacturer's protocol. The extracts were incubated at room temperature for 30 min in DNA binding buffer (10 mM Tris-HCl [pH 7.5], 150 mM NaCl, 5 mM DTT, 0.5% Tween-20) containing IRDye 700 (LI-COR Bioscience, Lincoln, NE, USA) labeled p53RE1 double-stranded oligomers annealed by p53RE1s and p53RE1as. In some experimental condition, non-labeled p53RE1 double stranded DNA oligomer or non-labeled p53RE1mt double stranded DNA oligomer (a product of annealing of p53RE1 mutant-s with p53RE1 mutant-as) were added to the extract with monoclonal anti-p53 antibodies, Pab421 and/or Pab1801. These oligomers are listed in Supporting information Fig. S1. The reactions were loaded on a 4% PAGE using 0.5 × TBE buffer and electrophoresed for 2 h at 120 V. The gels were scanned by the Odyssey infrared imaging system (LI-COR, Bioscience, Lincoln, NE, USA). Using SF126-tet-p53 cells, nuclear extracts were prepared under these conditions with or without p53 expression. The lower triangle indicates p53-p53RE1-Pab421 complex (sifted band). The upper triangle indicates p53-p53RE1-Pab421-Pab1801 complex (super-sifted band).

Fig. S4. Immunostaining for p53 and αB-crystallin. SF126 glioblastoma cells 1×10^4 were cultured directly on poly-D lysine coated Lab-Tek Chamber Slide (Nalge Nunc, Rochester, NY, USA) and transfected with pCR259-p53 (50 ng) or pCR259-cryab (150 ng). After 24 h, the cells were fixed with methanol-acetone (1:1) for 10 min at −20°C. Fixed cells were washed three times with PBS containing 0.05% Tween-20 (PBS-T). After blocking with PBS containing 5% skim milk at room temperature for 30 min, cells were incubated with anti-p53 (1:100 dilution) (DO-1; Santa Cruz Biotechnology, Santa Cruz, CA, USA) and anti-αB-crystallin (1:100 dilution) (SPA-223; Stressgen Biotechnology, Ann Arbor, MI, USA) antibodies. After washing with PBS-T, cells were incubated with Alexa Fluor 594-conjugated goat anti-rabbit IgG (1:400 dilution; Molecular Probes, Invitrogen, Carlsbad, CA, USA) and FITC-conjugated goat anti-mouse IgG (1:400 dilution; Molecular Probes). The stating cell was visualized on an LSM5 Pascal (Carl Zeiss, Göttingen, Germany). Green, p53; red, αB-crystallin.

Fig. S5. Overexpressed αB-crystallin stabilized p53. pCR259-p53 or pCR259-cryab was transfected in SF126 glioblastoma cells according to the indicated amount of plasmid with 100 ng of GFP expression plasmid. After 24 h transfection, cell lysates were immunoblotted using p53 and αB-crystallin or GFP antibodies. The relative expression level of p53 or αB-crystallin compared with GFP was analyzed using Kodak 1D Image Analysis Software (lower panel).

Please note: Wiley-Blackwell are not responsible for the content or functionality of any supporting materials supplied by the authors. Any queries (other than missing material) should be directed to the corresponding author for the article.